

# Using a 1D bandgap metamaterial to build up a delay line.

J Lucas\*, E Geron\*, T Ditchi†

Laboratoire de Physique et d'étude de la matière.

\* PSL Research University, ESPCI-ParisTech

† Sorbonne Universités, UPMC Univ Paris 06

CNRS UMR8213

F-75005 Paris, France

March 22, 2016

This paper is a postprint of a paper submitted to and accepted for publication in IET Microwaves, Antennas & Propagation and is subject to Institution of Engineering and Technology Copyright. The copy of record is available at IET Digital Library.

## Abstract

Classical lumped components delay lines are built with inductances and capacitors arranged as to match the standard telegraphist line model to obtain slow group velocity lines. In this paper we demonstrate that a practical way to obtain significant group velocity reduction consist in taking advantage of the forbidden bands that present a 1D meta-material. The feasibility of this kind of line, as well as its ability to transmit data are discussed and practically verified.

## 1 Introduction

The great historical application of delay lines is the radar application. They are used to separate the echoes of moving targets from the echoes of static objects such as the ground itself. Actually, long delays are obtained in radar applications by converting the radar frequency signal to optical signal which allows very long delays by making it propagate in wound optical fiber before converting it back to microwaves frequencies for processing. Another solution would consist in using shorter media where the velocity is much lower. Without dispersion, the only way to obtain a slow velocity in a line or a material consists in using high dielectric constant material. Unfortunately, without changing the nature of the waves as with SAW delay lines [1], only small velocity reduction can be obtained this way. It is possible though to obtain large velocity reduction by taking advantage of dispersion. Many applications are not wide band and are therefore compatible with smaller bandwidth. It is possible to obtain a significant velocity reduction in a medium over a limited bandwidth by taking advantage of some resonance. Many works based on this effect have been carried out such as in [2], or more recently in optics [3, 4, 5, 6]. In this paper, we propose to use the properties of bandgap metamaterial lines [7] to obtain the same result focusing on a propagation approach.

Firstly, we discuss the interest of relatively narrow bandwidth low group velocity line for delay line applications. We demonstrate how to calculate the required gain to obtain a given group velocity reduction using the Kramers-Kronig relations [8, 9, 10] and how it applies to 1D metamaterials. Then, we expose the theoretical key features that control the behavior of such lines : characteristic impedance, group velocity and bandwidth, and how they interact with each others. The design of the line is then tuned using a circuit simulation software [11] that allows to take into account the influence of the actual components implementation. At this point, the losses in both substrate and lumped components as well as impedance matching with standard  $50\ \Omega$  lines are taken into account. Finally the results obtained with a prototype are presented. The usability of such a system to obtain large delays is verified and discussed focusing on ability to transmit data.

## 2 Delay lines

An ideal electrical delaying device is a device whose frequency response is :  $H(\omega) = e^{-j\omega t_0}$ . In this equation,  $t_0$  is the delay,  $\omega = 2\pi f$  the circular frequency, and  $j = \sqrt{-1}$ . In the case of a line, the delay  $t_0$  is due to the propagation in the line and the frequency response can be rewritten as:  $H(\omega) = e^{-j\frac{\omega}{v}L}$ , where  $L$  is the dimension of the line and  $v$  a celerity which can be written as :  $v = \frac{L}{t_0}$ . As  $t_0$  and  $L$  are constants,  $v$  is a constant as well. This corresponds to a non dispersive medium.

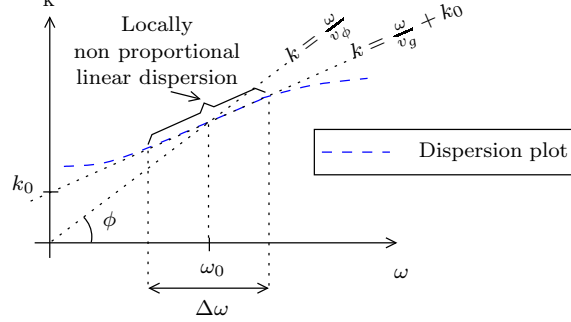


Figure 1: Non proportional linear dispersion over a limited bandwidth.

Nevertheless, if a limited bandwidth is acceptable as in the case of modulated signals for telecommunication or radar applications for instance, the delay line can be built using a media where the dispersion is linear:  $k = \frac{\omega}{v_g} + k_0$  and non proportional ( $k_0 \neq 0$ ) over the bandwidth as presented in figure 1 and where  $v_g$  is the group velocity defined as :

$$v_g = \frac{d\omega}{dk} \quad (1)$$

In that case, and if additionally the amplitude of the transmission coefficient remains constant in the bandwidth as in the Shustter model, it has been shown by Brillouin [12] that the propagation delay presented by the modulating signal is  $t_0 = \frac{L}{v_g}$  despite the phase velocity dispersion in the  $\Delta\omega$  frequency band.

Finally, to build up a delay line it is possible to use a media presenting a non proportional linear dispersion from 0 Hz up to the maximal frequency of the propagating signal, consequently where the phase and the group velocity are constant over this band. It is also possible to use a media where the dispersion is non proportional linear over a limited bandwidth and where only the group velocity is constant over the considered band. The classical delay lines are built according to the first method. In this paper, we focus on the second method.

### 2.1 Slowing down

Considering the Kramers-Kronig relations [8, 9], group velocity variations can be obtained by modifying the amplitude of the frequency response or transmission coefficient [10]. This is illustrated in figure 2. In this figure, curve (a) presents the relative targeted velocity variation of the group velocity, where  $v_0$  is the group velocity outside the frequency band where the velocity variation occurs. The shape of the velocity variation has been chosen arbitrarily. It is nevertheless important that the velocity variation remains bounded in frequency. In this figure, the frequencies are centered on  $f_0$ . By using equation 1, one can calculate the corresponding phase shift per length unit:

$$k(f) = \frac{2\pi}{v_0} \int \frac{1}{v_n(f)} df \quad (2)$$

In this equation,  $v_n(f) = \frac{v_g(f)}{v_0}$  which depends on  $\Delta f$ . figure 2b presents  $\frac{v_0}{c} (k(f) - k(f_0))$  where  $c$  is the speed of light in vacuum. This way, figure 2b is the same for all  $f_0$ . In this figure and later in the paper, 'lu' stands for length unit. It can be meters in continuous media or a number of elementary elements in discrete media.

Considering reference [10] p 7 (equation.18), with  $\mathcal{H}_T$  the Hilbert transform, one can obtain  $G(f)$  the modulus of the frequency response of a one unit long lossless line:

$$\frac{v_0}{c} \log(G(f)) = -\mathcal{H}_T \left( \frac{v_0}{c} \left( k(f) - \frac{2\pi f}{v_0} \right) \right) \quad (3)$$

$\frac{v_0}{c} \times G_{dB}$  is presented in figure 2c. Finally, one obtains the required gain  $G(f)$  that yields the expected velocity reduction for an electromagnetic wave propagating in a given direction along a line. Because the Hilbert transform of a constant is null, this result can be shifted by any constant. In this figure we have chosen to set the maximal value to zero dB. The data presented in this figure have been obtained for a maximal relative velocity variation  $\frac{\Delta v_{max}}{v_0}$  of 90 % and a velocity reduction bandwidth at half depth  $\Delta f$  of 100 MHz.

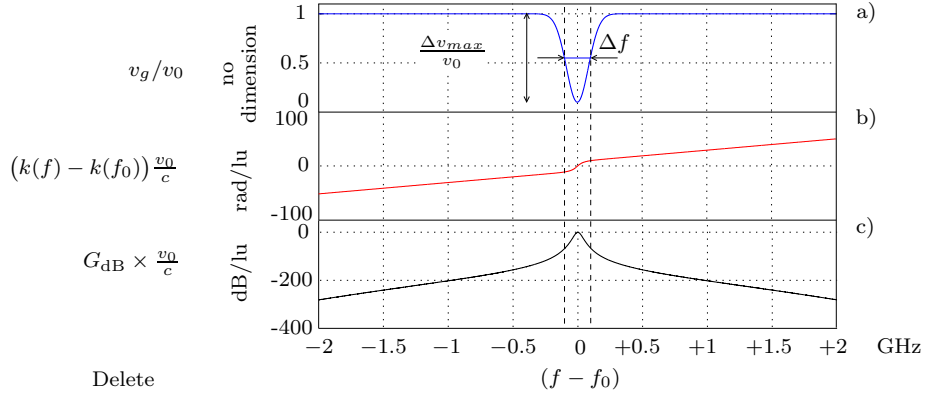


Figure 2: Targeted velocity reduction and corresponding gain variation.

**Losses** In the precedent paragraph we have not considered the losses. There are two main cases to consider. Whether the losses are constant with the frequency as it is the case with resistive losses, or they can be described with the constant loss angle approximation. In both cases, they simply superimpose to the gain modulus variation  $G(f)$  calculated with equation 3, without modifying the phase shift and thus the group velocity. Details about this point can be found in reference [10] pp 6-7.

## 2.2 Parametric variations

### Central frequency variation.

Let us calculate the effect of a frequency shift of the central frequency  $f_0$ . Let  $f_0 + f_{offset}$  be the new central frequency.  $f_{offset}$  can be positive or negative. The shifted velocity variation becomes :  $v_g(f - f_{offset})$ . In turn, with equation 2,  $k(f)$  becomes  $k(f - f_0)$ .

As the Hilbert transform is the convolution with  $\frac{1}{j2\pi f}$  and as the convolution is associative and that the Hilbert transform of a constant is null, the new required gain variation  $G_{offset}$  reads:

$$\begin{aligned} \frac{v_0}{c} \log(G_{offset}(f)) &= -\frac{1}{j2\pi f} * \left( \frac{2\pi}{v_0} k(f - f_{offset}) - \frac{2\pi}{v_0} f \right) \\ &= -\frac{1}{j2\pi f} * \left( \frac{2\pi}{v_0} k(f - f_{offset}) - \frac{2\pi}{v_0} (f - f_{offset}) + \underbrace{\frac{2\pi}{v_0} f_{offset}}_{\text{constant}} \right) \\ &= -\frac{1}{j2\pi f} * \left( \left[ \frac{2\pi}{v_0} k(f) - \frac{2\pi}{v_0} f \right] * \delta(f_{offset}) \right) \\ &= \frac{v_0}{c} \log(G(f)) * \delta(f_{offset}) \end{aligned} \quad (4)$$

In this equation  $\delta$  denotes the Dirac distribution and  $*$  is the convolution product. As one can see with this equation shifting the targeted velocity variation simply shifts the required gain. It does not change its amplitude.

As a conclusion to this paragraph, it is noticeable that it is the bandwidth of the velocity reduction  $\Delta f$  and not the quality factor  $\frac{f_0}{\Delta f}$  of the velocity reduction that is relevant as a parameter which is quite counter intuitive. Therefore, in the parametric study that follows, it is the velocity reduction bandwidth  $\Delta f$  that will be considered as a parameter.

### Bandwidth $\Delta f$ and velocity reduction factor $\frac{\Delta v_{\max}}{v_0}$ variations.

The results of figure 2 apply for any  $v_0$  and central frequency  $f_0$ . However they depend on the velocity reduction factor  $\frac{\Delta v_{\max}}{v_0}$  and on the velocity reduction bandwidth  $\Delta f$ .

We have computed the required gain  $G(f)$  for various values of  $\Delta f$  as presented in figure 3.

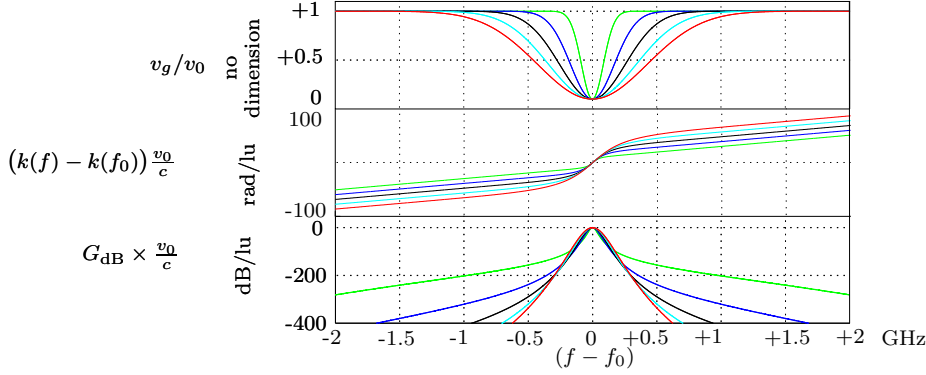


Figure 3: Influence of the bandwidth of the velocity reduction.

By doing so, and proceeding in the same way for various values of  $\frac{\Delta v_{\max}}{v_0}$ , one obtains the plots presented in figure 4. In figure 4a the variation of the required maximal value for  $G(f)$  as a function of the bandwidth is presented, when figure 4b presents the same parameter versus the relative velocity variation.

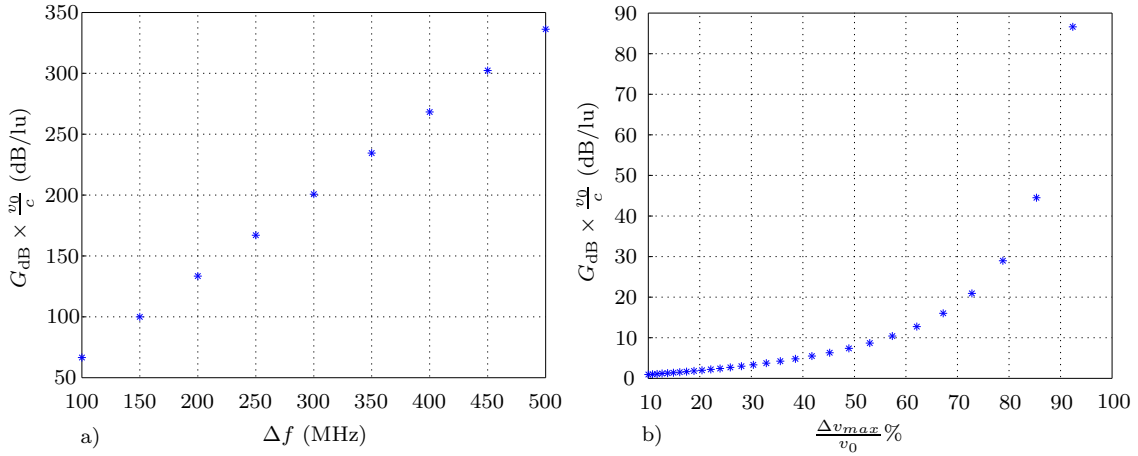


Figure 4: Influences of the bandwidth and relative velocity depth variation.

Considering figure 4b, one can see that it becomes very costly in terms of gain to reduce the group velocity beyond 90 %. In this work we targeted a velocity reduction of 90 %. figure 4a shows that the required gain is linear in dB. It actually increases exponentially. In section 2, we have seen that it is important to have a non proportional linear dispersion in order to allow band limited signal to propagate at the group velocity. One way to obtain this non proportional linear dispersion consists in working with a sufficiently large bandwidth compared to that of the transmitted signal.

## 2.3 Applications.

**Line approach:** By targeting a group velocity profile, one calculates naturally the characteristics a line should present: the wave vector and the gain per length unit. To obtain a given delay  $\Delta T$  one simply sets the length  $L$  of the line to  $L = v_g \cdot \Delta T$ . This is the great point about the line approach. Nevertheless, the precedent results can be applied only if the line segment is properly loaded so that there is only the incident wave to consider. It should be noted that setting the group velocity sets as well the characteristic impedance which as to be taken into account when building a prototype.

**Filter approach:** A system which exhibits the gain of figure 2c is a filter. It is indeed possible to obtain constant delay over a bandwidth with high order Bessel's filters. The order of the filter is related to the delay expected. It is always possible anyhow to split high order filter into a daisy chain of first and second order filters. It consists in fact in building a metamaterial line segment. In this paper we chose to use the line approach because it closely fits the metamaterial theoretical approach. It is particularly true in so far the impedance matching issue is concerned.

**Example of application:** In this paper, we consider as an example a telecommunication application around 2 GHz such as the DCS 1800 (Digital Cellular System) which is compliant with the GSM (Global System for Mobile Communications) protocol. The transmitted signals are narrow band to allow numerous transmission channels. A 100 MHz bandwidth allows to obtain a sufficiently non proportional linear dispersion around the central frequency for the typical channel width of the GSM protocol (200 kHz). Lets us use the results of the precedent section to estimate the required gain per length unit to obtain a group velocity reduction of 90%. With  $v_g \approx \frac{2}{3}c$  which is the group velocity in a  $50 \Omega$  coaxial cable, according to figure 4a, one has:  $\frac{v_g}{v_0} G_o \approx -66 \text{ dB/lu} \rightarrow G_0 \approx -100 \text{ dB/lu}$ . This corresponds to a very steep gain at the borders of the band. This can typically be achieved by the exponential attenuation between two forbidden band gaps in a metamaterial [7] or by using a resonant design as in reference [2]. This work is focused on the first technique because metamaterial allows to easily control  $\Delta f$  which is the relevant parameter of slow line design.

## 3 1D slow metamaterial lines

Electrical delay lines are classically build by cascading L-C cells as presented in figure 5a. Such lines are in fact a 1D metamaterial line. 1D metamaterial are made of elementary cells made of lumped components which, from an electrical point of view, are two ports circuits. Practically, the elementary cells and components are connected using line segments. Such material behave differently whether the propagation in the line segment can be neglected in front of the phase shift imposed by the lumped components or not. This is often referred as the sub-wavelength condition in the literature. In terms of material science, the 1D metamaterial line will be used in its first Brillouin zone [13] where the elementary cell length  $\ell$  is such that the line appears homogeneous to the electromagnetic wave it carries. This condition can be stated for instance as:

$$\ell < \frac{\lambda}{10} \quad (5)$$

where  $\lambda$  is the wave length of the carried wave.

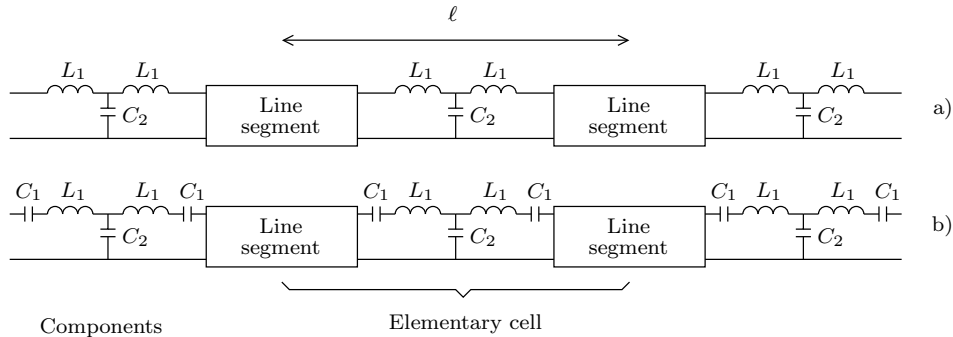


Figure 5: 1D Metamaterial slow lines: a) Classical LC line b) Band Gap Slow line

Under the sub-wavelength condition, only the lumped components are taken into account. Using Kirchhoff laws and Floquet's theorem, the phase shift per cell for an infinitely long line can be calculated. Equation 6 [14, 15] presents the theoretical dispersion for the classical LC structure of figure 5a.

$$\cos(\theta) = 1 - L_1 C_2 \omega^2 \quad (6)$$

In this equation,  $\theta$  is the phase shift per cell which can be complex. In sub wavelength condition, the length of the line  $L$ , as defined in section 2, is the number of cells, and one has:  $v_g = d\theta/d\omega$  in cells per seconds. With  $\ell$  the length of a cell it comes:  $v_g = d\theta/d\omega \cdot \ell$  in m/s. Considering the dispersion relation 6, waves are evanescent whenever  $|\cos(\theta)| > 1$ . Concurrently  $G(f)$  goes very low. With equation 6, one can calculate the corresponding modulus  $G(f) = |e^{-j\theta}|$  of the frequency response for one cell of an infinitely long line.  $G(f)$  for the classical LC structure is presented in dotted blue line in figure 6 along with the corresponding velocity. This kind of line is a low-pass structure. To make it work at 2 GHz as proposed in section 2.3 implies a very large bandwidth which is not favorable in so far velocity reduction is concerned as it is shown in figure 4a. In order to reduce this bandwidth we inserted a serial capacitor in the line to cut the low frequencies. The new line structure is presented in figure 5b. Equation 6 becomes [14, 15]:

$$\cos(\theta) = 1 + \frac{C_2}{C_1} - L_1 C_2 \omega^2 \quad (7)$$

$$f_1 = \frac{1}{2\pi\sqrt{L_1 C_1}} \quad (8)$$

$$f_2 = \frac{1}{2\pi}\sqrt{\frac{1}{L_1 C_1} + \frac{2}{L_1 C_2}} \quad (9)$$

One can see that the introduction the serial capacitor shifts up  $\cos(\theta)$ , thus creating a new bandgap that starts at zero Hertz. In DC condition,  $\cos(\theta) > 1$  because of the capacitor  $C_1$ . When the angular frequency gets greater than  $f_1$ , normal propagation occurs till  $\cos(\theta) < 1$  which corresponds to  $f_2$ . This behavior is summarized by the black solid curves in figure 6.

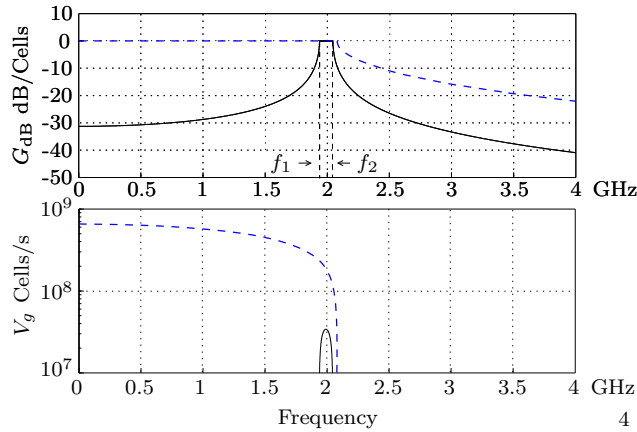


Figure 6: 1D slow line metamaterial behavior

This figure shows that there is, in the metamaterial, a propagation band flanked by two forbidden bands on each side. This reduces the band width and makes the slopes more steep. As expected from section 2.1, it reduces as well the group velocity in the pass-band.

It is possible to place  $f_1$  and  $f_2$  independently on the frequency axis. This allows to obtain the low propagation velocity presented in figure 6 at any frequency in sub-wavelength condition at the cost of the characteristic impedance. Indeed considering an infinity long line, it is also possible to calculate the characteristic impedance :

$$Z_c^2 = 2Z_1 Z_2 + Z_1^2 \quad (10)$$

where  $Z_1 = \frac{1}{j\omega C_1} + jL_1\omega$  and  $Z_2 = \frac{1}{jC_2\omega}$ . Setting  $v_g$  this is to say  $f_1$  and  $f_2$  consequently sets  $Z_c$ .

Finally, one has to find a compromise between velocity reduction and line impedance matching.

The velocity profile obtained in figure 6 is not the one considered in section 2.1. Indeed in this introductory section a media where the waves propagate for all frequencies was considered. In a band gap metamaterial, the waves only propagate in the pass-bands. Outside of this pass-bands the group velocity is infinite and has no particular physical signification and the wave vector modulus  $k$  is constant with  $k = n.\pi$  where  $n$  is an integer. It only varies in the pass-band. In both cases, the variation of the wave vector modulus  $k$  in these bands is positive as in the case considered in section 2.1. This of course leads in both cases to a corresponding required gain variation shaped as a pass-band. Further more in the case of a band gap metamaterial one can approximate the group velocity as:  $v_g \approx \frac{\Delta\omega}{\Delta k} = \frac{2\pi\Delta F}{\pi} = 2\Delta F$  in cells per seconds. This further illustrates the general results of equation 4 which states that  $\Delta F$  is the relevant parameter. Finally as band gap metamaterial makes it possible to control  $\Delta F$ , they are an excellent way for building slow lines.

## 4 Tuning the slow line

In this work, the targeted frequency is about 2 GHz (see section 2.3), therefore equation 5 yields  $\ell < 1$  cm when using microstrip lines over a PTFE woven glass substrate. This condition can be respected using classical hybrid technology [16]. Consequently, the 1D metamaterial components values are calculated in a first time without considering the line segment using equations 8 and 9. The design is then post corrected to take into account the inherent serial inductance of the line segments, which adds to  $L_1$ , and parallel capacitance which adds to  $C_2$ . They are both assumed to be small to bring only minor corrections.

In the realization presented hereafter we have chosen to favor velocity reduction over characteristic impedance. One can find in Table 1 the values calculated to obtain a bandwidth of about 100 MHz around 2 GHz. In the same table, one will find as well, the values corrected by simulating [11] a line of 10 cells of the metamaterial. It practically corresponds to a 7 cm long line taking into account the line segments used to practically build the line.

	Theoretical values without line segment	Corrected values with line segment
$L_1$	4.5 nH	3.4 nH
$C_1$	1.5 pF	1.4 pF
$C_2$	26 pF	21 pF

Table 1: Values calculated using equation 7 and post corrected by simulation for the 1D slow metamaterial line.

The obtained line presents a low characteristic impedance of about  $3 \Omega$  which makes it necessary to use quarter wave line segments at its input and output in order to avoid reflections. As these quarter wave line segments are not slow line segments, the multiple reflections they induce are short lived compared to the propagation time in the line itself and do not perturb the line propagation of the signal. This point will be verified with the transient measurements of section 5.2.

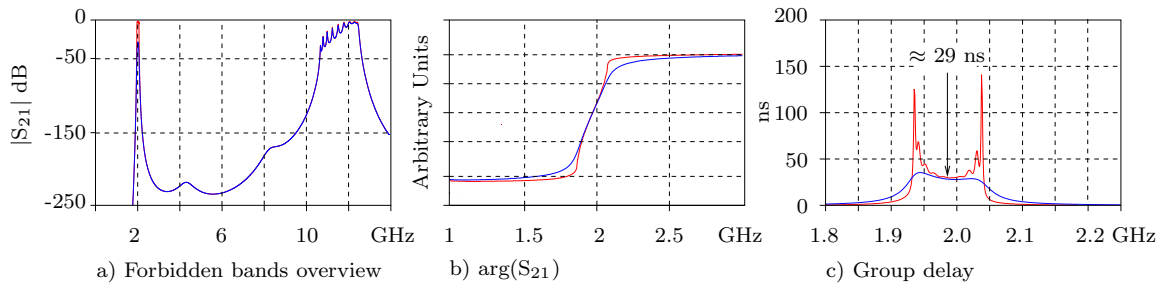


Figure 7: Simulated slow line forbidden bands and performances. Without losses (red). With losses (blue)



figure 7a presents an overview of the behavior of the transmission for a 10 cells line. It exhibits a narrow passband with very steep slopes around 2 GHz as required to significantly reduce the group velocity. When the frequency goes higher a second passband appears. It corresponds to the second Brillouin zone when the “classical” propagation cannot be neglected because the condition of equation 5 is no longer respected. The phenomenon that creates this pass-band is the classical Bragg effect. figure 7b presents the shape of the argument of the transmission coefficient, which shows that there is indeed a strong variation of the group velocity in the considered passband. Finally, figure 7c presents the corresponding group delay. The 29 ns at the center of the band are to be compared to the  $\approx 0.35$  ns that would be obtained in a classical 12 cm long microstrip line, which is the length of the prototype.

## 5 Building and characterizing the slow line

### 5.1 Realization

The line calculated and simulated has been realized and is presented in figure 8. In this figure, one can see the 1D metamaterial line between its two quarter wave length tapered lines. These lines realize the impedance matching between the  $50\ \Omega$  connectors and the  $3\ \Omega$  metamaterial line. The  $12\ \Omega$  required for the quarter wave length lines makes them very large compared to the metamaterial line, which is the reason why they gradually increase and decrease at each end to avoid a potentially mismatching step. One can see as well that the connection to the ground is realized through a top side ground plane whose equipotentiality is ensured by multiple vias to the bottom ground plane. The zoom on one of the cells details the practical implementation the line. One may notice the use of a  $2L_1$  inductor and two  $C_1$  capacitors which allows to maintain the cell symmetry while reducing the number of lumped components.

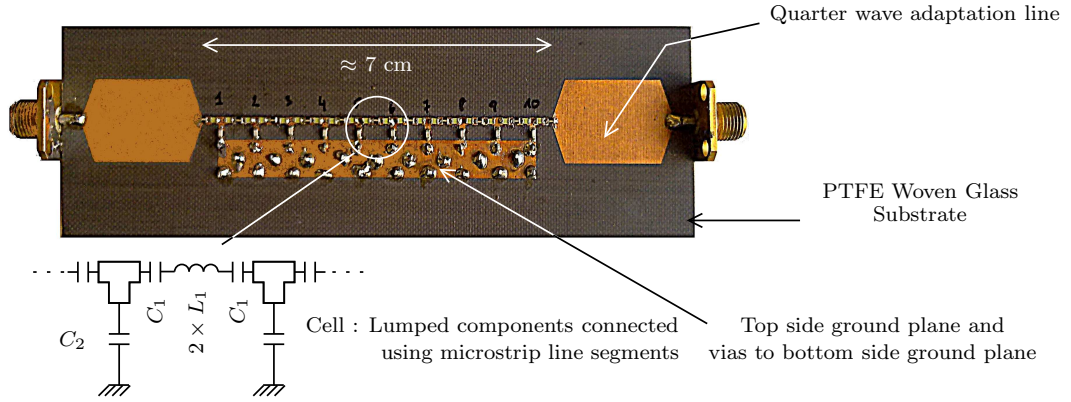


Figure 8: The slow line prototype.

### 5.2 Performances

We have firstly measured the value of the group velocity and group delay for the prototype. This measurement was simply realized using a Vector Network Analyzer (VNA) to measure the transmission coefficient  $S_{21}$ . This corresponds to a steady state measurement. The corresponding group delay  $GD$  and group velocity  $v_g$  can be obtained with equations 11 and 12:

$$GD = 2\pi \left( \frac{dS_{21}}{df} \right)^{-1} \quad (11)$$

$$v_g = L/GD \quad (12)$$

where  $L=12$  cm is the total length of the prototype.

The results are presented in figure 9. They are narrow band compared to the simulation which allows to properly calibrate the VNA. One can see that as long as the amplitude of  $|S_{21}|$  is sufficiently large, they are comparable to



the simulation results presented in figure 7. By measuring the group velocity using a linear regression as presented in figure 9a, the velocity reduction ratio is 35 as presented in Table 2.

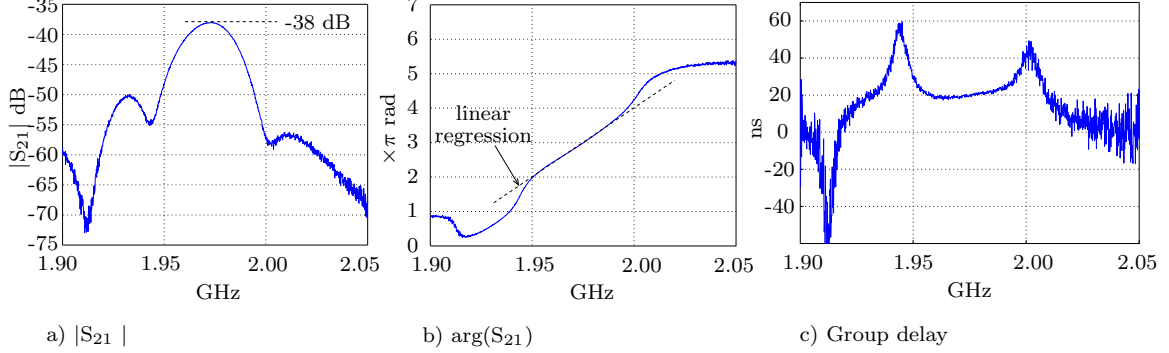


Figure 9: Steady state Measurement of the slow line performances.

The attenuation (-38 dB) is quite strong and comparable to the simulation where the measured losses of each kind of components was used. We can conclude that it is mostly due to the components. At this level, these losses prevent of course to use such a line for industrial applications. Nevertheless it allows to validate the concept. Though being high, the losses do not prevent to measure the effective data transmission ability of the slow line.

	$V_{g_{ref}}$	$V_{g_{Slow}}$	$\frac{V_{g_{ref}}}{V_{g_{Slow}}}$	Reflection ( $ S_{11} $ )	Losses
Simulated	$2.06 \cdot 10^8$ m/s	$4.20 \cdot 10^6$ m/s	48	-15 dB	-29 dB
Steady State measurement (via VNA $S_{21}$ )	$2.1 \cdot 10^8$ m/s	$5.99 \cdot 10^6$ m/s	35	-10 dB	-38 dB
Transient measurement (Zero span SPA)	$2.14 \cdot 10^8$ m/s	$5.84 \cdot 10^6$ m/s	37	**	-40 dB

\*\* = Not measured

Table 2: Summary of the performances of the slow line.

We have verified the ability of the built up slow line to effectively transmit data at slow velocity. To do so, we measured the effective signal velocity by comparing the transit time of a Gaussian filtered CPFSK ( Gaussian Frequency Shift Keying ) [17] modulated data frame in the slow line to the one in a reference microstrip line of the same length. By doing so, we are sure to effectively measure the information velocity, which would have not been fully the case if we had used a Gaussian modulated signal for instance [18]. The experimental setup is presented in figure 10.

A data set, chosen to easily recognize its middle bit, is used to modulate a carrier at the central frequency of the slow line. The GFSK modulator generates a synchronization signal. The modulated signal alternatively propagates in the slow line and in a microstrip line of the same overall length which is used as reference measurement. After its transit in the slow line, or in the reference line, the signal is demodulated using a Spectrum Analyzer (SPA) in zero span mode with the same settings in both cases (reference level, resolution filter, sweep time). This way we verified that the information is correctly transmitted, and we measured the effective delay for the information introduced by the slow line. The middle bit is identified inside the data frame by demodulating the whole frame. Its start date is measured as the middle of the rising time in both cases. This method for measuring the information velocity is insensitive to any bias that would result from some deformation of the signal. The velocities measured this way can be found in Table 2 and confirm the possibility to use the slow line to transmit data.

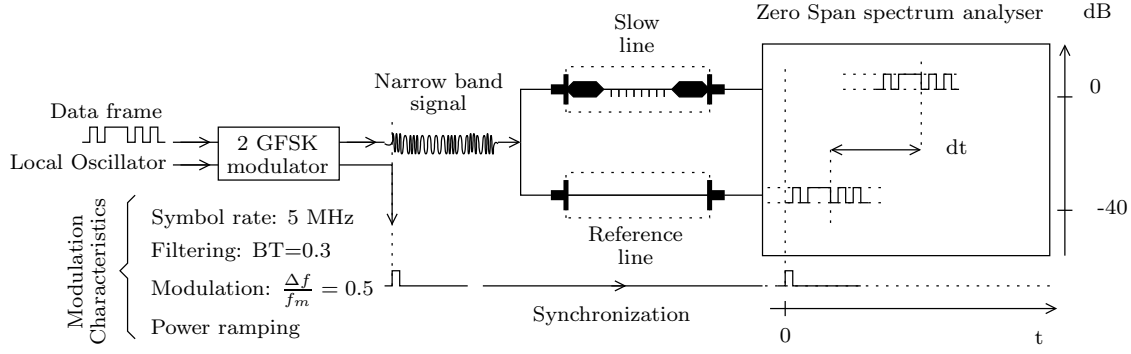


Figure 10: Experimental signal velocity measurement setup.

## 6 Conclusion

In this work, after having studied the possibilities to delay a signal and verified that a low group velocity is a possible method, we have demonstrated that a bandgap material permits to obtain significant velocity reduction efficiently. A parametric study along with theoretical considerations have allowed us to determine that it is the velocity reduction bandwidth  $\Delta f$  and the velocity reduction factor that are the relevant parameters to design the line. The theoretical study of a 1D hybrid bandgap metamaterial has shown that it can be used to obtain the expected performances. Simulation have allowed us to optimize the metamaterial line for real implementation. A prototype has been realized using hybrid technology and presents strong losses in spite of the use of PTFE woven glass substrate. We have verified by simulation, after having measured the power dissipated in the components, that the lost power is not radiated nor reflected. The prototype presents the expected performances in terms of bandwidth and group velocity in steady state conditions. In order to verify that the variations of the transmission coefficient magnitude do not prevent, by distorting the signal, to actually use the line to transmit data, we have tested the data transmission capability. We thus verified that the prototype allows data transmission at the expected low velocity. Thus any delay could be obtained by increasing the number of cells. Consequently realizing such delay line should present an effective alternative to the use of optical fibers if realized using Monolithic Microwave Integrated Circuit (MMIC) technology.

## References

- [1] M. B. Schultz and M. G. Holland. Surface acoustic wave delay lines with small temperature coefficient. *Proceedings of the IEEE ISSN:0018-9219*, 58(9):1361–1362, 1970. DOI 10.1109/PROC.1970.7928.
- [2] S. Lucyszyn and D. Robertson. Analog reflection topology building blocks for adaptive microwave signal processing applications. *IEEE Transactions on Microwave Theory Tech.*, MTT-43(3):601–611, March 1995.
- [3] M. Junker. Adapting brillouin spectrum for slow light delays. *Electronics Letters*, 43:682–683(1), June 2007.
- [4] Toshihiko Baba. Slow light in photonic crystals. *Nature photonics*, 2(8):465–473, 2008. doi:10.1038/nphoton.2008.146.
- [5] Luc Thévenaz. Slow and fast light in optical fibres. *Nature photonics*, 2(8):474–481, 2008. doi:10.1038/nphoton.2008.147.
- [6] Dowlett Darell, Thierry Ditchi, Emmanuel Geron, and Jerome Lucas. Operational Slow Line Underpinned by a 1D Metamaterial. In *Proceeding PIERS in Tapei*, March 2013.
- [7] S. Tretyakov. Contemporary notes on metamaterials. *IET Microwaves, Antennas and Propagation*, 1:3–11(8), February 2007.
- [8] R. Kronig de Laer. On the theory of dispersion of x-rays. *J. Opt. Soc. Am. Rev. Sci. Instrum.*, 12:547–557, 1926.

- [9] C.F Bohren. What did Kramers and Kronig do and how did they do it? *Eur. J. Phys.*, 31:573–577, 2010. doi:10.1088/0143-0807/31/3/014.
- [10] J Lucas, E Géron, T Ditchi, and S Holé. A fast Fourier transform implementation of the Kramers-Kronig relations: Application to anomalous and left handed propagation. *AIP Advances*, 2, 032144-1, 2012. <http://dx.doi.org/10.1063/1.4747813>.
- [11] ADS Simulation software. Technical report, Agilent technologies, 2012.
- [12] L. Brillouin. *Wave Propagation and group velocity*. Academic Press INC, 1960. pp. 7-9, Library of Congress catalog card number: 59-13829.
- [13] L.Brillouin and M.Parodi. *Propagation des ondes dans les milieux périodiques*. Masson TE cie Dunod, 1956.
- [14] G.V. Eleftheriades and K.G. Balmain. *NEGATIVE-REFRACTION METAMATERIALS*. IEE Press Wiley-Interscience, 2005. pp. 95-97, ISBN 13: 978-0-471-60146-3.
- [15] Christophe Caloz and Tatsuo Itoh. *Electromagnetic Metamaterials: Transmission Line Theory and microwave applications/The Engineering Approach*. Wiley Interscience, 2006.
- [16] E. Géron, T. Ditchi, J. Lucas, and S. Holé. Electronically controlled asymmetric microstrip line coupler underpinned by an hybrid right-left-handed line. *IET Microwaves, Antenas & Propagation*, August 2012. doi: 10.1049/iet-map.2011.0426.
- [17] C. Jordan. *Reference Data for Engineers 7th edition*, chapter 24. Howard W.S SAM & COMPANY, 1989. ISBN: 0-672-21563-2.
- [18] T. Sauter. Gaussian pulses and superluminality. *J. Phys. A: Math. Gen.*, 35:6743–6754, 2002. PII: S0305-4470(02)34090-3.